JOURNAL OF PROPULSION AND POWER
Vol. 33, No. 5, September–October 2017

Potential of Variable-Geometry Method for Compressor Range Extension for Turbocharged Engines

Qiangqiang Huang* and Xinqian Zheng†
State Key Laboratory of Automotive Safety and Energy, Tsinghua University, 100084 Beijing, People's Republic of China

DOI: 10.2514/1.B36004

Increasingly stringent requirements on fuel economy and emissions are propelling turbocharging technology to improve the power density of engines. In the future, turbocharged engines with ultrahigh-power density must be equipped with high-pressure compressors. However, the narrow stable operating range of a compressor at a high-pressure ratio is always a restriction. The variable-geometry method, which refers to the combination of a variable-inlet prewhirl and variable diffuser vanes in this paper, will be a preferred choice for the range extension of compressors, and so estimating its potential for range extension is of long-term value. This paper investigated the performance of a centrifugal compressor adopting the variable-geometry method via a steady three-dimensional Reynolds-averaged Navier–Stokes simulation. The combination of variable diffuser vanes, ranging from −10 to 10 deg, and a variable-inlet prewhirl, ranging from −20 to 60 deg, has the potential to improve the stable operating range from 23.5 to 63.0% at a pressure ratio of 4.8. The corresponding increase in the low-end engine torque is estimated to be 53%. The combination shows advantages in terms of operating range and efficiency performance over only adjusting the diffuser vanes or simply changing the inlet prewhirl. The contributions from the variable-inlet prewhirl and variable diffuser vanes to the shifts of the surge line and choke line are discussed as well.

Downloaded by TSINGHUA UNIVERSITY on October 11, 2017 | http://arc.aiaa.org | DOI: 10.2514/1.B36004

Nomenclature

A	=	throat area
$B_{d,x}$	=	blockage factor at the diffuser throat, in which x denotes the throat and d denotes the diffuser
c	=	absolute velocity
c_p	=	specific heat capacity at constant pressure
D	=	diameter
D_2	=	diameter at the impeller outlet
H_u	=	fuel low heating value
i	=	incidence
Mu_2	=	tip-speed Mach number, $U_2/\sqrt{\gamma RT_{01}}$
$\dot{m}$	=	mass-flow rate of air
$\dot{m}_{d,c}$	=	diffuser choking mass flow
$\dot{m}_{i,c}$	=	impeller choking mass flow
N	=	rotational speed
P_{et}	=	engine effective power output
p	=	pressure
R	=	stable operating range
T	=	temperature
T_{tq}	=	torque
u	=	impeller blade-tip velocity
W	=	relative velocity
w	=	angular velocity
α	=	prewhirl angle or air–fuel ratio
γ	=	specific-heat ratio
η_{et}	=	effective engine efficiency
η_i	=	impeller adiabatic efficiency, which is calculated from the inlet to the rotor/stator interface
ρ	=	density
ϕ	=	flow coefficient, $\dot{m}/(\rho_1 N D_2^3)$
ψ	=	pressure-rise coefficient, $\Delta P/(\rho_1 N^2 D_2^2)$

Subscripts

c	=	choke
d	=	diffuser
i	=	impeller
s	=	surge or engine shaft
u	=	circumferential component
w	=	working
x	=	position of throat
z	=	axial component
0	=	total parameter
1	=	impeller inlet
2	=	rotor/stator interface

Received 13 September 2015; revision received 19 November 2016; accepted for publication 6 May 2017; published online 27 July 2017. Copyright © 2017 by the American Institute of Aeronautics and Astronautics, Inc. All rights reserved. All requests for copying and permission to reprint should be submitted to CCC at www.copyright.com; employ the ISSN 0748-4658 (print) or 1533-3876 (online) to initiate your request. See also AIAA Rights and Permissions www.aiaa.org/randp.

*Master Candidate, Department of Automotive Engineering, Turbomachinery Laboratory; hqq14@mails.tsinghua.edu.cn.

†Associate Professor, Department of Automotive Engineering, Turbomachinery Laboratory; zhengxq@tsinghua.edu.cn (Corresponding Author).

I. Introduction

THE variable-geometry method, which aims at helping a compressor operate at an operating point with the desired performance by adjusting the geometric settings, has been widely adopted by many compression applications. For gas-turbine compressors or industrial compressors, which usually work continuously for long times, the variable-geometry method can ensure a relatively high-efficiency operation, even under off-design conditions or inlet fluctuations. For aeroengine compressors, which often operate in complex environments or under transient conditions, such as startup and shutdown, the method is often used to suppress flow instabilities, such as surge or rotating stall, and to enhance the stable operating range. In other words, the variable-geometry method makes a compressor operate efficiently over a wide range.

In axial compressors, the variable-geometry method generally involves variable-inlet guide vanes (VIGVs) and variable stator vanes [1]. In centrifugal compressors with vaned diffusers, the variable-geometry method is usually implemented using VIGVs and variable diffuser vanes [2]. Depending on the operating conditions, the stagger angles of these vanes are adjusted by mechanical linkages outside the pressure-containing body. The gaps between the impeller and diffuser vanes can also be adjusted [3,4].

Turbocharger compressors, which are usually centrifugal, play a significant role in developing more powerful, cleaner, and more economical internal combustion engines. For an engine working at high altitudes, the compressor delivering a high-pressure ratio (PR) is able to maintain constant inlet manifold pressure and ensure efficient combustion in the engine [5]. For diesel engines, which are heavily restricted by increasingly stringent emission regulations, the high-

Downloaded by TSINGHUA UNIVERSITY on October 11, 2017 | http://arc.aiaa.org | DOI: 10.2514/1.B36004

pressure intake that accompanies high exhaust-gas recirculation can reduce NO_x and soot emissions simultaneously [6]. For the gasoline engine, by adopting new technology, such as the Miller cycle to improve fuel economy, high-PR compressors are employed to compensate the volumetric efficiency [7]. However, the operating range of a compressor is limited by the surge line, especially at high PRs. With a left shift of the surge line or an extension of the operating range, the low-end torque of an engine can also be improved. With the development of turbocharging technology, an important issue that remains to be solved is the extension of the compressor operating range.

The variable-geometry method can be an effective way to widen the operating range of a turbocharger compressor. Especially for a compressor with a vaned diffuser, which usually has an efficiency advantage over that with a vaneless diffuser, the variable-geometry method can make up for the shortcoming of a reduced operating range. In the future of high boosting technology, the compressor that uses the variable-geometry method will be a preferred choice for automotive industries. As mentioned earlier, VIGVs and variable diffuser vanes are the representatives of the variable-geometry method for turbocharger compressors.

Mohtar et al. [8] and Herbst et al. [9] validated the range-extension effect of VIGVs on a turbocharger compressor through experiments and simulations, respectively. In Herbst et al.'s work, a vane angle of 20 deg leads to a reduction in surge mass flow of up to 21%. Coppinger [10] and Mohseni et al. [11] investigated the influence of the configurations of the inlet guide vanes (IGVs) and flow passage. It was found that the performances with different configurations were quite different. Actually, the objective of using VIGVs is just to implement a variable-inlet prewhirl, which means that the circumferential component of the velocity of the inlet flow is nonzero and can be adjusted. Inlet radial vanes [12,13], reinjecting rotating gas [14], and inlet volute [15] can also be used to achieve a variable-inlet prewhirl. To avoid the influence of the specific type and configuration of the swirl generator, this paper exploits the inlet boundary condition of a velocity direction to implement a variable-inlet prewhirl.

Oatway and Harp [16] presented a comprehensive review on the flow-control method for the range extension of turbocharger compressors, and their experimental results indicated that, between the 110 and 45% diffuser-throat areas, a flow range (the operating range to the surge flow) of approximately 3.5:1 was achieved without excessive efficiency penalty at a PR of 2.4, and so they conclude that using variable diffuser vanes is the most practical method for extending flow-range control. Variable diffuser vanes directly influence the component performance and the matching between the diffuser and the impeller, which will definitely change the surge flow, choking flow, and performance. A numerical research also showed the effectiveness of variable diffuser vanes on widening the operating range [17]. An experimental research done by Ubben and Niehuis [4] showed that the clearance between the vanes and the wall of the diffuser influences the operating range; however, there is no recommendation or standard for the width of the clearance at present. Additionally, because the clearance is between solid bodies, it can be quite small. Therefore, in this paper, the clearance is always assumed to be zero.

Much research has been done on a variable-inlet prewhirl and variable diffuser vanes separately, but there has been little investigation on their combination. Simon et al. [18] adjusted an inlet prewhirl and diffuser vanes simultaneously for centrifugal compressors. The combination proves to offer efficiency improvement over the entire operating range compared with using only a variable-inlet prewhirl or variable diffuser vanes. Furthermore, the authors also suggested how to determine the optimal combinations of diffuser and prewhirl angles for the purpose of efficiency improvement. Their work emphasizes the efficiency benefit brought by the combination of different variable-geometry methods. However, the potential of variable-geometry methods for extending the operating ranges of compressors has not been determined quantitatively, and the corresponding improvements in low-end engine torque are still unclear as well. These predictions are very important when evaluating the necessity of employing the variable-geometry method. The differences between the variable-inlet prewhirl and variable diffuser vanes, and their combination for the purpose of range extension have not been reported comprehensively. A comparison over a wide speed range and vane-angle range will be valuable to a decision maker when constructing a technology road map.

The potential for range extension through a variable-inlet prewhirl has been studied in [19]. If an inlet prewhirl manages to greatly change the performance map, what is the mechanism for the change? Previous research answered this question and explained how the positive inlet prewhirl shifted the surge line and choke line. However, a variable-inlet prewhirl may not always influence the performance map significantly. After combining a variable-inlet prewhirl with variable diffuser vanes, whether the potential will be enhanced greatly or only slightly is still a question. We can look at this issue in another way by considering the effectiveness of a variable-inlet prewhirl for compressors with different diffuser vane angles. Actually, it turns out that, if a variable-inlet prewhirl is applied after closing the diffuser, the contribution from the variable-inlet prewhirl to the range extension is relatively limited. Thus, in this paper, some discussion about a variable-inlet prewhirl on when the effects of the variable-inlet prewhirl will be significant is given.

In this paper, we focus on the variable-geometry method, which is the combination of a variable-inlet prewhirl and variable diffuser vanes. The main body consists of three parts. First, the numerical methods are stated and validated. In the second part, the performances of a centrifugal compressor with different degrees of prewhirl and diffuser vanes are shown, and then the contributions from the variable-inlet prewhirl and variable diffuser vanes to the shifts of the surge line and choke line are discussed. Third, the corresponding improvement in the low-end torque of the engine from applying the variable-geometry method is estimated.

II. Flow Modeling and Simulation Procedure

A. Investigated Compressor and Meshing

The compressor-geometry model is shown in Fig. 1a. It consists of a vaned diffuser and an impeller with splitters. Each vane can be rotated around the middle point of the centerline by 10 or −10 deg. Table 1 shows the detailed configuration of the compressor. Because the geometry is axisymmetric, only one impeller passage and one diffuser passage were meshed, as shown in Fig. 1b. The side surfaces of the mesh were periodically matched. The total number of nodes is approximately 1.05 million, and the mesh of the impeller uses 0.88 million nodes. The grid independence has been validated in our previous work [20]. The width of the cells nearest the wall is 0.002 mm. The shroud gap of the impeller is 0.5 mm. The clearance in the diffuser was not meshed.

B. Numerical Methods

The commercially available code NUMECA FINE/Turbo was employed to solve steady Reynolds-averaged Navier–Stokes equations. The central scheme and the fourth-order Runge–Kutta scheme were selected for spatial discretization and temporal discretization, respectively. The Spalart–Allmaras single-equation model was used as the turbulence model. The width of the first layer of cells, 0.002 mm, ensured that y^+ was below 10 in all simulations of this paper, which must be satisfied for modeling the viscous sublayer in the turbulence model [21]. The rotor/stator interface was modeled using the full nonmatching mixing-plane method. An open test case of the compressor, Radiver [22], was used to validate the numerical method. The measurements on Radiver were carried out at the Institute of Jet Propulsion and Turbomachinery at RWTH Aachen University, Germany. Part of the investigation was funded by the Deutsche Forschungsgemeinschaft. Radiver is a single-stage centrifugal compressor with a vaned diffuser. The steady and unsteady experimental results of the test case were published. The compressor geometry, figures, animations, and supplementary information have been compiled for the test case. The diffuser on the test rig is adjustable, and data for different setups of diffuser vanes

Downloaded by TSINGHUA UNIVERSITY on October 11, 2017 | http://arc.aiaa.org | DOI: 10.2514/1.B36004

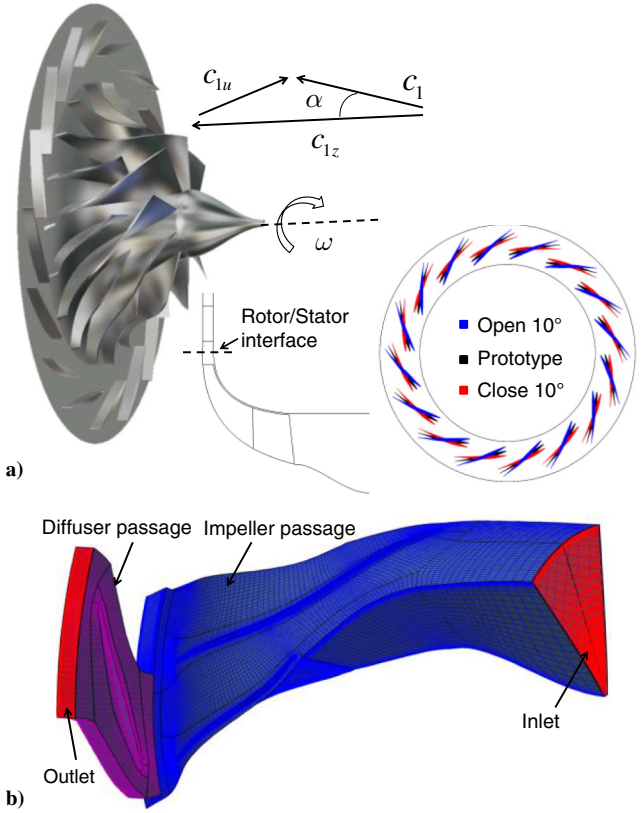

Fig. 1 a) Compressor model; b) mesh.

have been released. The numerical validation was conducted with the setup, in which the diffuser-vane angle is equal to 16.5 deg, and the ratio between the diffuser inlet radius and the impeller outlet radius is 1.14. The grid size of the single-passage mesh of the compressor is 2 million. The simulation results show that y^+ near the wall is lower than 10 in the whole field, which satisfies the requirement for turbulence modeling.

Performances and flowfields from experimental tests and simulations are compared at 80% design speed, as most of the published experimental data are at this speed. The computed choking mass flow at 80% speed is 2.278 kg/s, which differs from the experimental choking mass flow of 2.191 kg/s. This implies that the effective throat area was slightly overestimated by the simulation. The overestimation of choking flow is ascribed to the turbulence model, which greatly influences the development of the boundary layer and the tip clearance, which may change with rotational speed. After the mass-flow rates are normalized using the choking mass flows from tests and simulations, it turns out that the simulation results have a good agreement with the test results on most of the parameters, as shown in Figs. 2 and 3. The compressor efficiency and PR characteristics are well captured by the simulation, which proves the fidelity of the simulation for predicting compressor performance. The efficiency is calculated from the impeller inlet to the diffuser outlet. To examine the ability of the simulation to capture flow

Table 1 Compressor parameters

Parameters	Value and unit
Design rotational speed N	111,700 rpm
Impeller outlet diameter D_2	1.00×10^2 mm
Tip-speed Mach number Mu_2	1.69
Total PR at the design point	5.50
Flow coefficient at the design point ϕ	0.004
Pressure-rise coefficient at the design point ψ	0.003
Impeller throat area A_i	1.74×10^3 mm^2
Diffuser-throat area A_d	5.67×10^2 mm^2

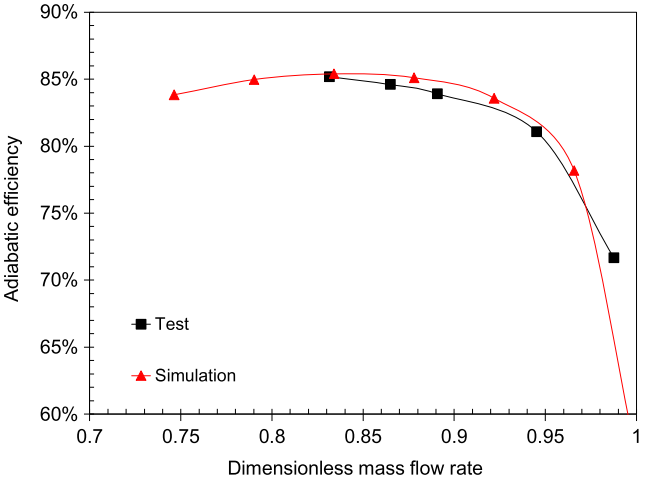

Fig. 2 Adiabatic efficiency performances of the compressor Radiver from tests and simulations.

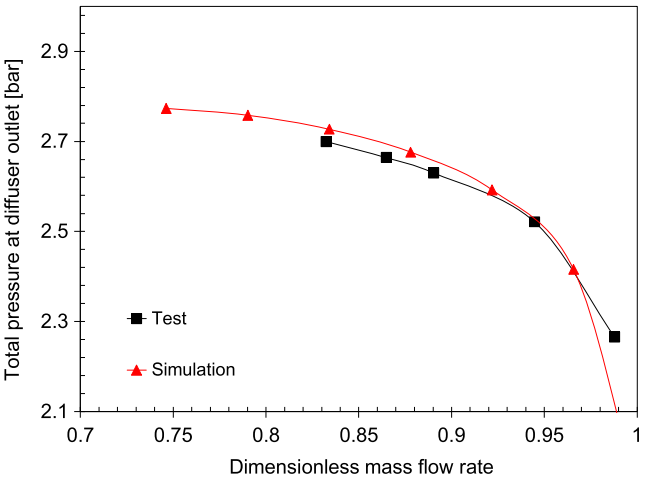

Fig. 3 Total pressure at the diffuser outlet of the compressor Radiver.

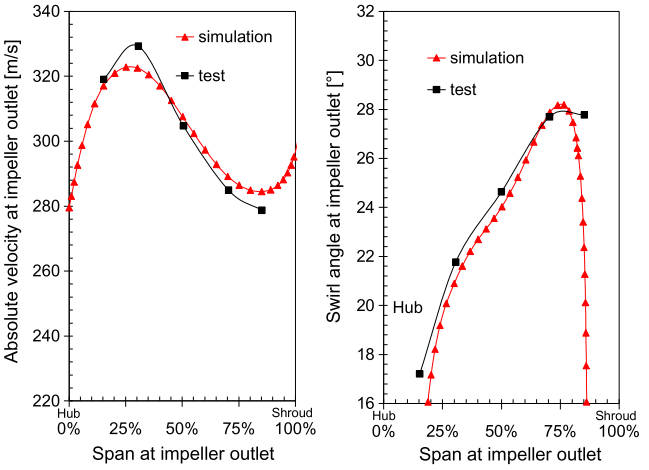

Fig. 4 Absolute velocity and swirl angle at the impeller outlet of the compressor Radiver.

features, at the operating point where the dimensionless mass-flow rate is equal to 0.83, spanwise plots of quantities at the impeller outlet are shown in Fig. 4. Figure 5 shows the flowfields at the diffuser inlet, which validates the agreement between the tests and the simulations. The magnitudes of the velocity and the swirl angle are successfully predicted. Additionally, via simulation, quantity distributions at the

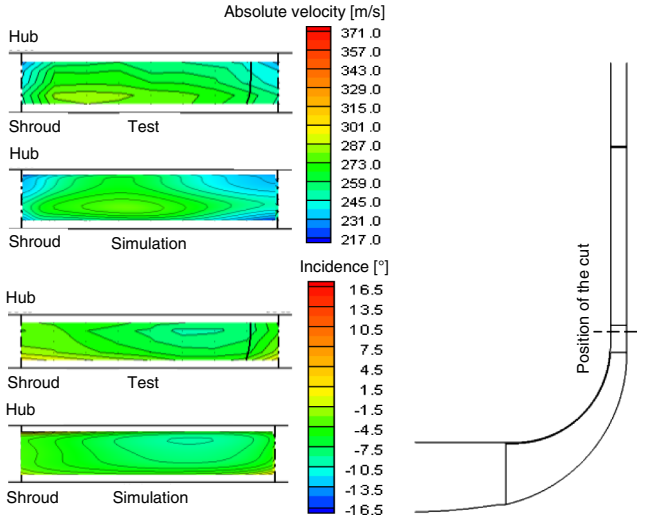

Fig. 5 Absolute velocity and incidence near the diffuser inlet of the compressor Radiver.

impeller outlet and diffuser inlet are captured. To sum up, the numerical methods used in this paper have been validated for investigating the performance and flow features.

C. Simulation Procedure

For the inlet boundary condition, the inlet prewhirl angle was set by the velocity direction, and the absolute total pressure and total temperature were 101.325 kPa and 298.15 K, respectively. No-slip and impermeability conditions were imposed on all solid surfaces. Simulations were conducted at 100, 90, 80, 60, and 40% maximum speed. Because the peak points of the pressure characteristics provide a convenient engineering approximation for the surge limit, the peak PR point of each speed line was taken as the surge point. The authors are not saying that flow instabilities, such as surge and rotating stall, occur at the maximum PR points based on steady computations. Compressor-performance maps with different geometric setups were simulated, producing a large amount of data. To compare the stable operating ranges for all the cases, the use of the maximum PR point as the left end of each compressor characteristic is a reasonable compromise.

III. Extending the Stable Operating Range of the Compressor

A. Performance and Range Extension

The computed mass-flow rate at the design point is 0.48 kg/s. As shown in Fig. 6a, both closing of the diffuser and positive prewhirl can shift the surge line left, at the expense of a PR drop. When the PR is above 2.2, the shift becomes quite obvious. Compared with the case "close 10 deg," the combination of closing the diffuser and positive prewhirl shifts the surge line more to the left at PRs above 4.0. Figure 6b shows the right shifts of the choke line that are induced by the variable-geometry method. At 90% speed and below, opening the diffuser significantly increases the choking flow. At 80% speed and above, the effect of a negative prewhirl on the choking flow is very obvious. For the case of combining negative prewhirl and opening of the diffuser, the choking flow is increased at all speeds. Especially at 80 and 90% speed, the increase resulting from the combination is much greater than that resulting from only opening the diffuser or only imposing negative prewhirl. The stable operating range R is defined by Eq. (1). Figure 6c shows the extended range resulting from the combined effect of the variable-inlet prewhirl from −20 to 60 deg, and variable diffuser vanes from −10 to 10 deg. At the PR of 4.8, the combined variable-geometry method increases R from 23.5% (i.e., 1–0.39/0.51) to 63.0%.

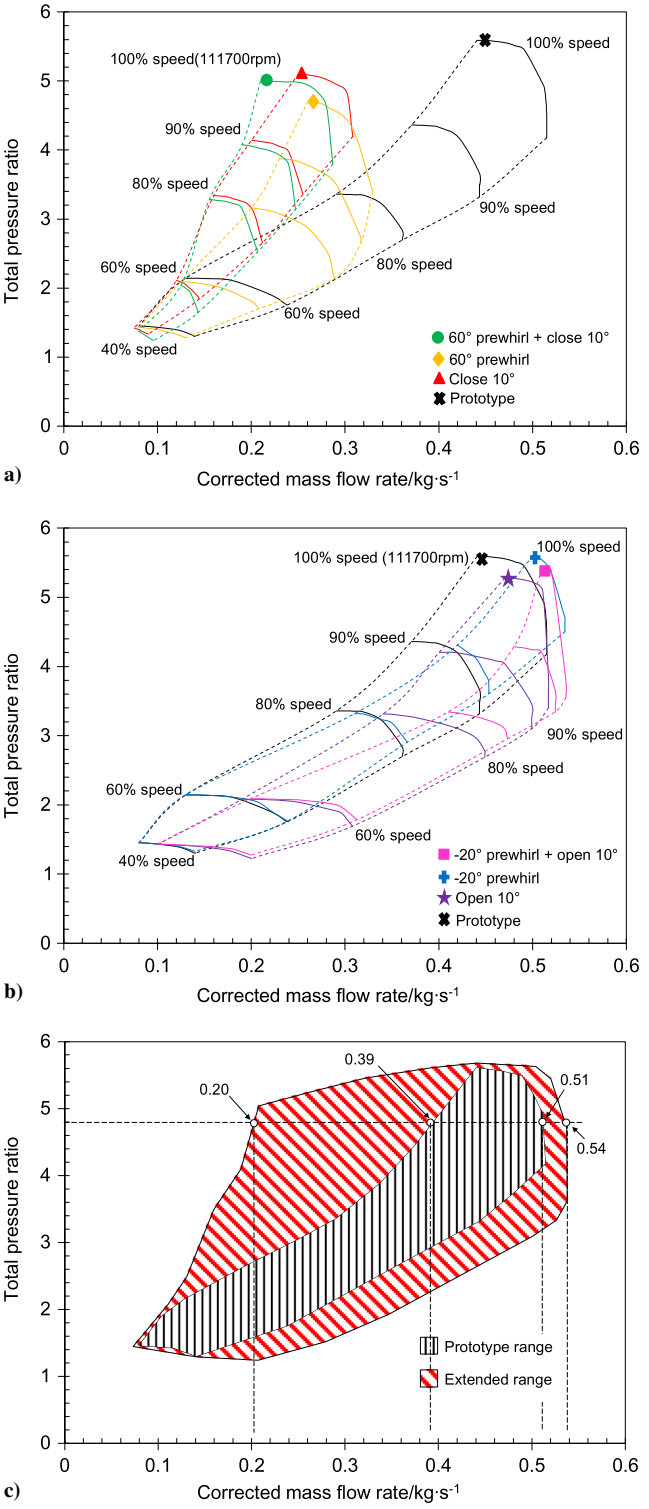

Fig. 6 Compressor-performance maps and range extension.

$$R = \left(1 - \frac{\dot{m}_s}{\dot{m}_c}\right)_{\mathrm{PR=const}} \times 100\% \tag{1}$$

Actually, the benefits of the combined variable-geometry method lie not only in widening the flow range, but also in improving efficiency. As shown in Fig. 7, the efficiency performance resulting from the combination is higher than that resulting from only closing the diffuser. For instance, for a given operating point at which the PR is 4.0 and the mass flow is 0.23 kg/s, the combined variable-geometry method and close 10 deg both can achieve high efficiency at

Downloaded by TSINGHUA UNIVERSITY on October 11, 2017 | http://arc.aiaa.org | DOI: 10.2514/1.B36004

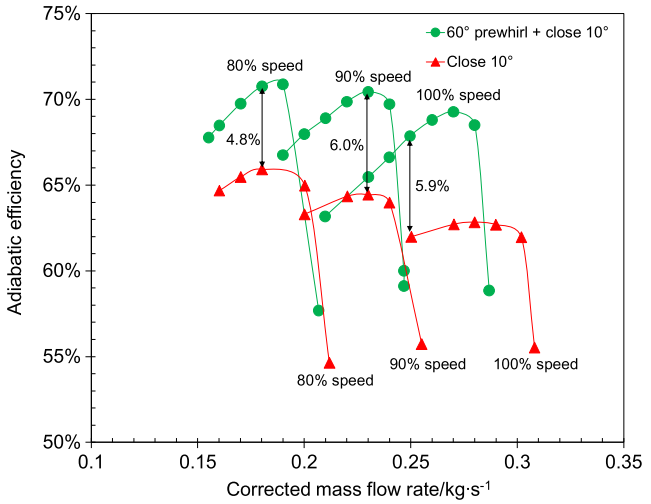

Fig. 7 Efficiency improvement by using variable-geometry method.

90% speed, but the combined variable-geometry method has an advantage of 6.0 points in efficiency.

Closing the diffuser forces the impeller to operate at the left branch of the efficiency characteristic, which heavily exacerbates impeller performance. As shown in Fig. 8, the impeller efficiency of close 10 deg is quite low. After exerting a positive inlet prewhirl, the performance of the diffuser almost does not change, but the impeller efficiency increases significantly. Thus, the positive inlet prewhirl compensates for the poor impeller performance caused by closing the diffuser. As shown in Fig. 9, the separation vortex of 60 deg prewhirl + close 10 deg at the inducer inlet is much smaller than that of close 10 deg. At a given mass-flow rate, a positive inlet prewhirl can reduce the Mach number and incidence at the impeller inlet, which has been proved through analyzing the velocity triangle in Fig. 10. Thus, a positive inlet prewhirl relieves the heavy flow separation at the inducer inlet, which directly reduces the entropy increase there and contributes to improving the impeller efficiency. Furthermore, an inlet prewhirl was shown to be able to adjust the matching relation between the impeller and the diffuser [23,24], which greatly contributes to the shift of the impeller characteristic and the efficiency gains.

An experimental work done by Simon et al. [18] also proved the efficiency benefits arising from combining these two variable-geometry methods, in which the IGV was installed, the diffuser could be replaced, and there was no volute. The authors concluded that, in their case, the efficiency gains with a combined adjustment amount to approximately 2% and up to 6%; these gains are similar in magnitude to the efficiency gains in this paper. This paper may estimate the

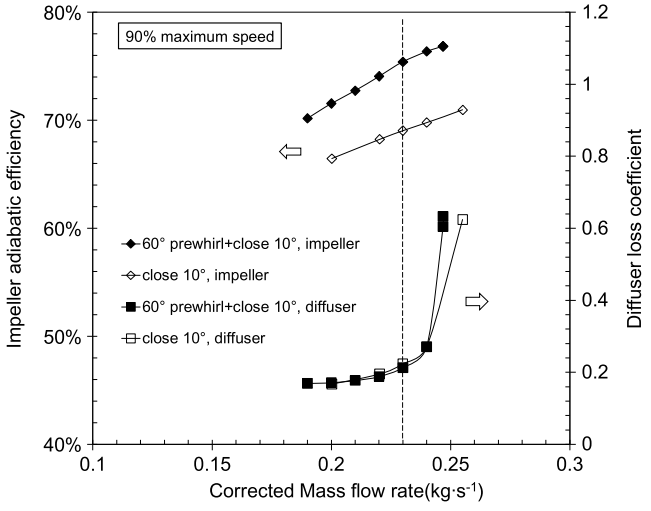

Fig. 8 Impeller adiabatic efficiency and diffuser loss coefficient.

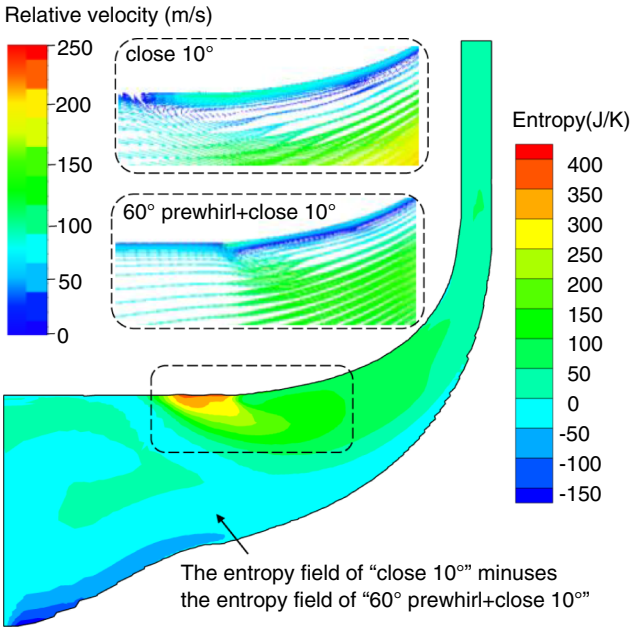

Fig. 9 Entropy contour and relative-velocity contours.

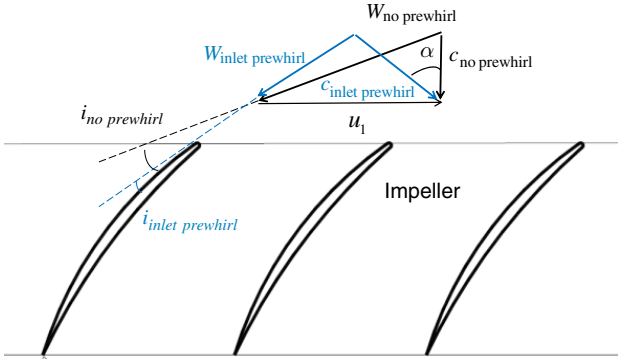

Fig. 10 Velocity triangle at the impeller inlet.

potential of the combined variable-geometry method for improving efficiency. On the other hand, the authors think that flow loss of inlet guide vans, deviation of the prewhirl angle, leakage flow in the clearance between the adjustable vanes and the diffuser wall, and the interaction between the diffuser and the volute may affect the efficiency performance. These negative aspects could result in an efficiency improvement that is not as high as our estimate for the combined geometry method. In the future, the penalty estimations from these effects should be discussed in the case of combining both variable-geometry methods. It is worthwhile investigating how to reduce their impacts on performance.

B. Discussion on the Shift of Surge Lines

Whether the impeller or the diffuser triggers flow instability in the prototype will be determined, which is the basis for analyzing the influences of the variable-geometry method on the surge line. It is inferred that flow instability is triggered by the impeller when the PR is below 2.2 in the prototype, that is, the rotational speed is lower than 60% maximum speed. At 60% speed, closing the diffuser, which makes the diffuser operate more stably, does not result in a significant displacement of the surge line toward lower flow, and so it is not the diffuser that controls the surge flow at 60% speed. However, at 80% speed, closing the diffuser causes the surge line to move considerably to the left, which indicates that the diffuser triggers flow instability at 80% speed. From the point of view of the matching between the

Downloaded by TSINGHUA UNIVERSITY on October 11, 2017 | http://arc.aiaa.org | DOI: 10.2514/1.B36004

impeller and the diffuser, the diffuser will become larger for matching as the rotational speed increases [25], which means the diffuser characteristic would tend to lie in the higher mass-flow region compared with the impeller characteristic. Thus, it is reasonable to infer that the diffuser triggers flow instability at 80% speed and above, which leads to the left shift of the surge line at PRs above 2.2 through the closing of the diffuser.

To provide more insight for the flowfield at maximum PR points, streamlines and pressure on blade surfaces are shown in Fig. 11. At 100 and 80% speeds of datum case, circulation is found between the impeller outlet and the diffuser inlet, although its area in the meridional views is relatively small. These circulations, which are due to curvature effect, considerably affect flow stabilities at the diffuser [26]. Because of the change of matching relation between the impeller and the diffuser at 80% speed, the impeller tends to operate at a more unstable region, which is indicated by a larger separation vortex near the inducer tip. After closing the diffuser by 10 deg, the separation vortex in the inducer grows larger and extends out of the impeller tip. However, 60 deg prewhirl relieves the extent of the separation vortex in the inducer, which benefits flow instabilities in the impeller and drives the impeller to work at a lower surge mass flow.

The contribution from variable diffuser vanes on the shift of the surge line has been discussed earlier, and the effect of the variable-inlet prewhirl will be discussed in the following section.

As shown in Fig. 6a, the positive inlet prewhirl fails to shift the surge line of the prototype to the left at PRs below 2.2, and it also fails to shift the surge line of close 10 deg at PRs below 4.0. In the experimental research done by Rodgers [27], the IGV angle of 27 deg fails to make the surge line move to the left at PRs below 3.7, which shows a similar trend with our results. The low mass flow and low inlet relative Mach number at the surge point are the two reasons for the ineffectiveness of the positive inlet prewhirl.

The inlet prewhirl influences the characteristics of components and their matching. However, if the choking flow of the compressor is too small, the effects of the positive inlet prewhirl are also small. With some assumptions (one is that the efficiency of the impeller is 100%), Zheng et al. [23] showed that the positive inlet prewhirl influences the choking flows of the impeller and the diffuser, as in Eqs. (2) and (3), respectively, in which $\dot{m}_{i,c}$ is the choking flow of the impeller, $\dot{m}_{d,c}$ is the choking flow of the diffuser, and c_{1u} is the circumferential component of the inlet velocity. Therefore, if the choking flow of the impeller or the diffuser is very small, the change in the choking flow by the inlet prewhirl is also very small. For the prototype at PRs below 2.2 (i.e., at 40% speed and 60% speed) and for the case of close 10 deg at PRs below 4.0 (i.e., at 90% speed and lower speeds), the influence of the inlet prewhirl on the shifts of characteristics is negligible, and so the shifts of the surge lines are also not significant. This is the so-called ineffectiveness of the inlet prewhirl caused by the low mass flow at the surge point.

$$\frac{\partial \dot{m}_{i,c}}{\partial c_{1u}} = \frac{-3\dot{m}_{i,c}u_1}{c_pT_{01} - c_{1u}u_1 + (u_x^2/2)} \tag{2}$$

$$\frac{\partial \dot{m}_{d,c}}{\partial c_{1u}} = \frac{-3\dot{m}_{d,c}u_1}{c_pT_{01} - c_{1u}u_1 + u_2^2} \tag{3}$$

The inducer stall plays an important role in the instability of the impeller performance. The complex interaction between the shock wave and the boundary layer, which may cause the increase of blockage, can aggravate the inducer stall [28]. As indicated by Fig. 10, the positive inlet prewhirl is able to relieve the relative Mach number at the inducer inlet. Especially when the relative Mach number approaches unity, the relief resulting from the positive inlet prewhirl will contribute significantly to stabilizing the performance of the impeller and the left shift of the surge line. Figure 12 shows the relative Mach-number fields at the surge points where the surge mass flows will reduce obviously after the positive inlet prewhirl is exerted (see Fig. 6a). In both of the fields, there are regions where the relative Mach number exceeds unity. After exerting the positive inlet prewhirl, the stability of the impeller will be improved. As shown in Fig. 13, the slope of the impeller PR characteristic at the surge point of

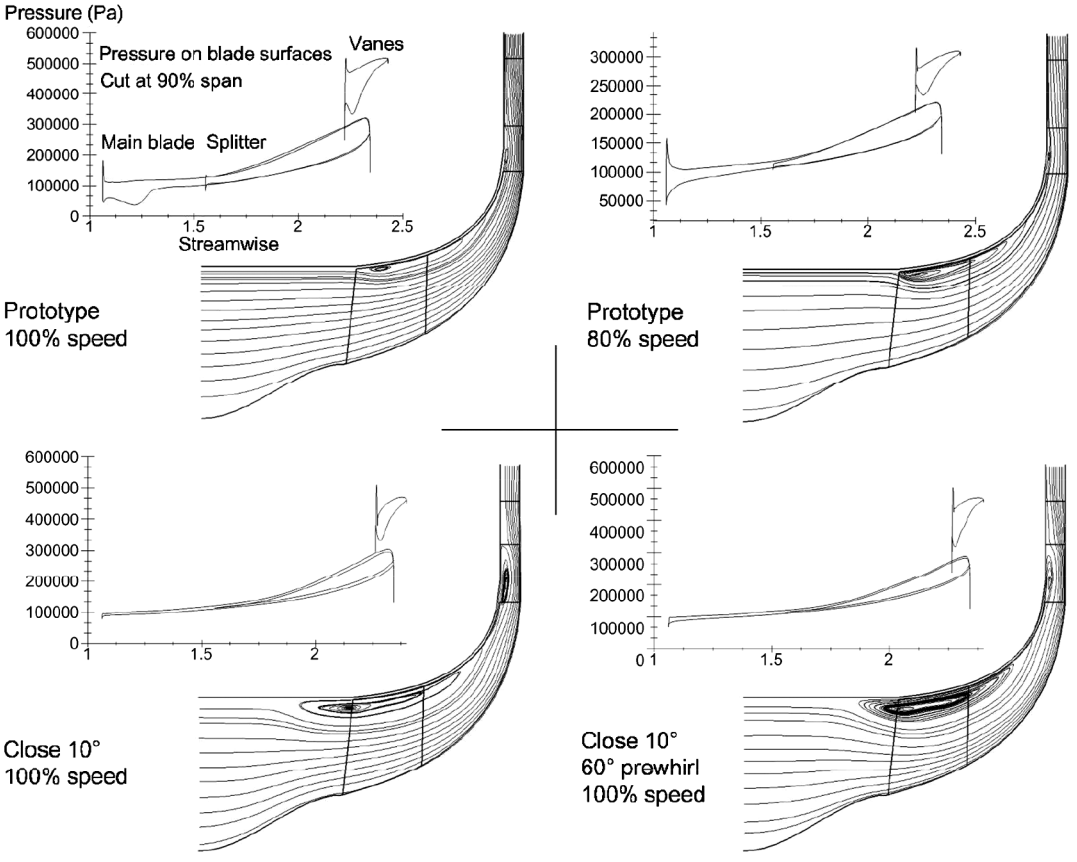

Fig. 11 Streamlines in the meridional views and pressure distributions at the peak PR points.

Downloaded by TSINGHUA UNIVERSITY on October 11, 2017 | http://arc.aiaa.org | DOI: 10.2514/1.B36004

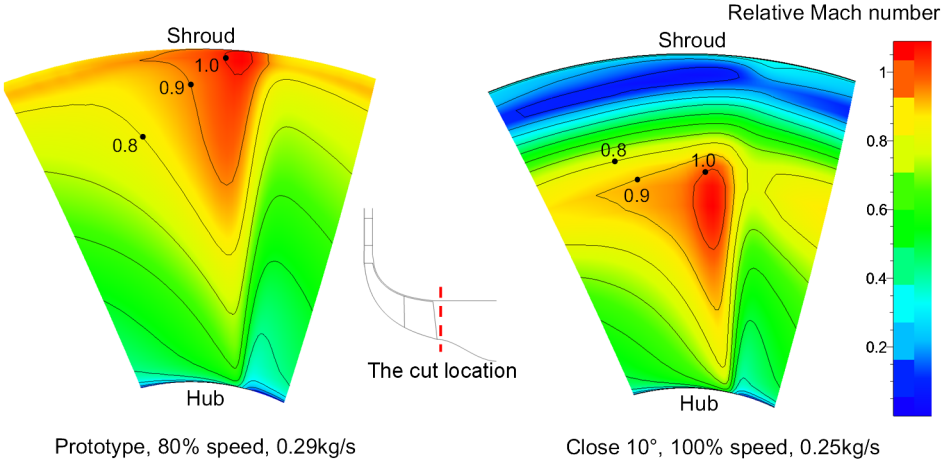

Fig. 12 Relative Mach-number contours with supersonic area in the inducer.

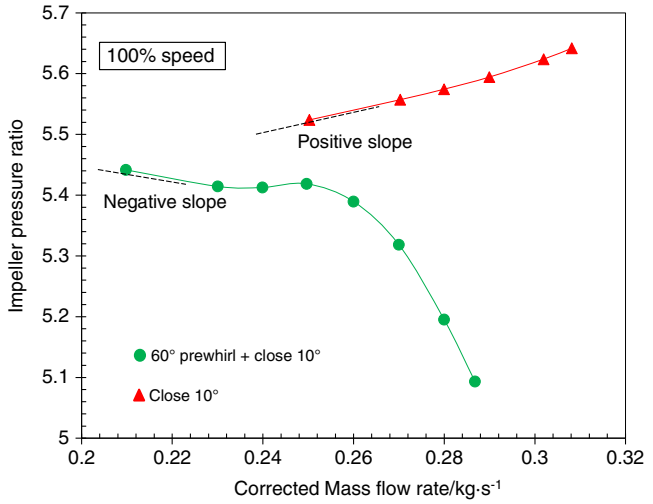

Fig. 13 Impeller PR characteristics.

close 10 deg is positive, which indicates the high instability of the impeller. However, the slope at the surge point with 60 deg inlet prewhirl and the closing of the diffuser vanes by 10 deg becomes negative, which proves that the relief of the excessive relative Mach number by the positive inlet prewhirl does stabilize the impeller performance. Figure 14 shows the relative Mach-number fields at the surge points where the surge mass flows are barely reduced after the positive inlet prewhirl is exerted (see Fig. 6a). In both of the fields, there are no supersonic regions. It seems that the positive inlet prewhirl is ineffective for reducing surge flow if the relative Mach number at the inducer inlet does not exceed unity. This is the so-called ineffectiveness of the inlet prewhirl, caused by the low inlet relative Mach number at the surge point.

C. Discussion on the Shift of Choke Lines

Opening the diffuser vanes by 10 deg enlarges the throat area of each diffuser from 5.67×10^2 to 7.68×10^2 mm^2, but only increases the choking flow at 100% speed from 0.515 to 0.517 kg/s, which implies that the diffuser controls the choking flow at 100% speed for the prototype and that the choking flow of the impeller is just slightly larger than that of the diffuser. The choked component turns out to be the impeller after opening the diffuser, and so the increase of the choking flow is not proportional to and is much less than the increase of the throat area of the diffuser.

As shown in Fig. 10, inlet prewhirl means that the velocity of fluids at the compressor inlet has a non-zero circumferential component. Therefore, work input from the impeller would decrease according to the Euler equation [26]. Because the inlet prewhirl can adjust the work input into the fluid, the total temperature and the total pressure at the throttle would usually drop with the positive inlet prewhirl, and rise with the negative inlet prewhirl, which cause changes in the choking mass flow. Zheng et al. [23] investigated the influence of the inlet prewhirl on the matching between the impeller and the diffuser. If the impeller and diffuser are supposed to match well in the case of zero inlet prewhirl, they will become mismatched in the case of nonzero inlet prewhirl. With the positive inlet prewhirl, the throat area of the diffuser is too large for the matching impeller. An intuitive corollary is that the throat area of the diffuser is too small for the matching impeller in the case of the negative inlet prewhirl. Thus, after imposing negative prewhirl, the diffuser is too small for a good matching and the compressor must still be choked at the diffuser at 100% speed. As shown in Fig. 15, the compressor with −20 deg prewhirl is choked at the diffuser, as the static pressure on the rotor/stator interface and near the diffuser inlet does not vary with the static pressure imposed at the outlet. Opening the diffuser greatly increases the stage choking flow at 90% speed and below, because the diffuser is always controlling the choking flow at these speeds. As shown in Fig. 16, if negative prewhirl is imposed, the compressor with an open diffuser is still choked at the diffuser at 90% speed.

Although the inlet prewhirl has been proven to influence choking mass-flow rates in many cases in Fig. 6, the choking mass-flow rates barely change with the inlet prewhirl in some cases, such as close 10 deg at 90% speed and prototype at 60% speed. Table 2 shows the choking mass-flow rates for which the inlet prewhirl has almost no impact on the choking mass-flow rate. To reveal the mechanism, first, this problem should be analyzed from the one-dimensional perspective, and then plots of corresponding parameters should be shown in support of the explanation. As described in the last paragraph, the compressor is choked at the diffuser in these cases, and so a basic choking mass-flow equation of the diffuser is presented as Eq. (4). By applying the ideal gas law and the sonic-speed equation, Eq. (4) can be rearranged into Eq. (5). Taking the impeller-efficiency equation, Eq. (6), into account, the choking mass-flow-rate equation, Eq. (7), is obtained. T_{02} is the total temperature at the rotor/stator interface, which is used to measure work input. $B_{d,x}$ and η_i are the blockage factor at the diffuser throat and the impeller efficiency, respectively. These three aerodynamic factors considerably influence the choking mass-flow rates. Figure 17 shows that the inlet prewhirl does change the work input. For instance, in the case of close 10 deg at 90% speed, 60 deg prewhirl reduces T_{02} by 27 K at the mass-flow rate of 0.25 kg/s, which should greatly affect the choking mass-flow rate. However, because 60 deg prewhirl also helps to improve impeller efficiency by 5.8 points, as shown in Fig. 8, and the diffuser performance almost never changes, 60 deg prewhirl does not change the compressor choking mass-flow rate. The same situation occurs in the case of the prototype at 60% speed. Although −20 deg prewhirl increases the work input, the impeller performance is worsened and

Downloaded by TSINGHUA UNIVERSITY on October 11, 2017 | http://arc.aiaa.org | DOI: 10.2514/1.B36004

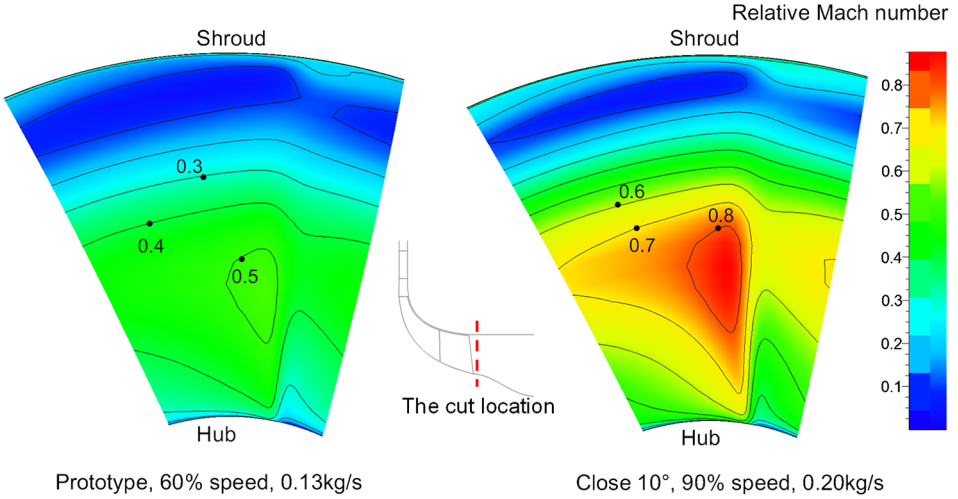

Fig. 14 Relative Mach-number contours without supersonic flow in the inducer.

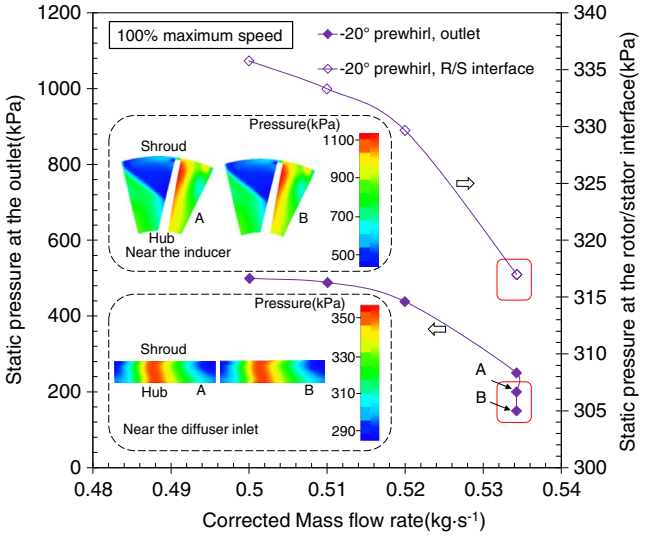

Fig. 15 Static-pressure distributions of the choking points at the maximum speed.

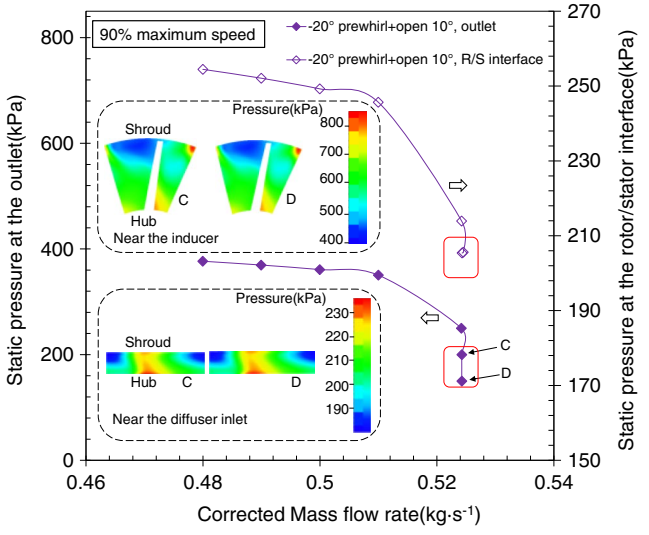

Fig. 16 Static-pressure distributions of the choking points at 90% speed.

the diffuser performance does not change, as shown in Figs. 18 and 19, which keeps $B_{d,x}$ the same and causes η_i to decrease. The influences of these three factors counteract one another, and so the compressor choking mass-flow rate remains 0.24 kg/s.

$$\dot{m}_{d,\text{choke}} = \rho_{02} a_{02} B_{d,x} A_{d,x} \left(\frac{2}{\gamma+1}\right)^{(\gamma+1)/(2\gamma-2)} \tag{4}$$

$$\dot{m}_{d,\text{choke}} = \rho_{01} a_{01} B_{d,x} A_{d,x} \left(\frac{T_{02}}{T_{01}}\right)^{-(1/2)} \frac{p_{02}}{p_{01}} \left(\frac{2}{\gamma+1}\right)^{(\gamma+1)/(2\gamma-2)} \tag{5}$$

$$\frac{p_{02}}{p_{01}} = \left[1 + \frac{\eta_i (T_{02} - T_{01})}{T_{01}}\right]^{(\gamma/(\gamma-1))} \tag{6}$$

$$\dot{m}_{d,\text{choke}} = \rho_{01} a_{01} B_{d,x} A_{d,x} \left(\frac{T_{02}}{T_{01}}\right)^{-1/2} \left(\eta_i \frac{T_{02}}{T_{01}} - \eta_i + 1\right)^{(\gamma/(\gamma-1))} \times \left(\frac{2}{\gamma+1}\right)^{(\gamma+1)/(2\gamma-2)} \tag{7}$$

IV. Improving the Low-End Torque of an Engine

Here, a rough estimation of the ability of the variable-geometry method to improve low-end engine torque is obtained (in a way similar to [19]). Figure 20 shows two compressor working lines at low engine-shaft speeds. One is for the prototype and the other is for the compressor employing the variable-geometry method. The surge margin (SM) is defined by Eq. (8) [26], and it is controlled above 12% in this study. The corner point of a working line has the greatest risk of flow instability, and so it also represents the highest boost level that a compressor delivers to an engine at low speeds. W and W' are the corner points of the working lines in the original range and extended range, respectively. S is the surge point at the same rotational speed of W. S' is the corresponding surge point of W'. The SM of W is 13.1% and that of W' is 16.0%. Both of the working lines almost hit the

Table 2 Choking mass-flow rates in selected cases

Case description	Inlet prewhirl, deg	Choking mass-flow rate, kg/s
Close 10 deg at 90% speed	0	0.26
	60	0.25
Prototype at 60% speed	0	0.24
	−20	0.24

Downloaded by TSINGHUA UNIVERSITY on October 11, 2017 | http://arc.aiaa.org | DOI: 10.2514/1.B36004

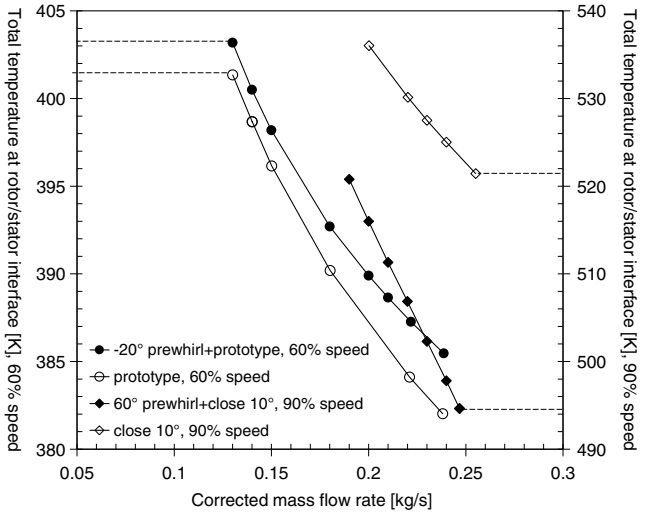

Fig. 17 Total temperatures at rotor/stator interface in selected cases.

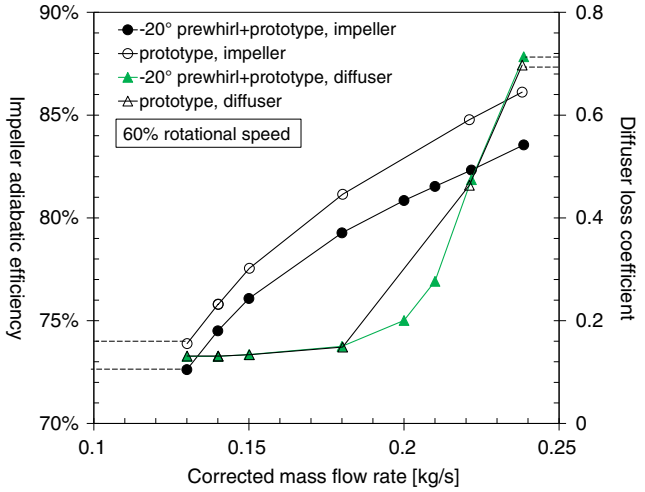

Fig. 18 Impeller adiabatic efficiency and diffuser loss coefficient at 90% speed.

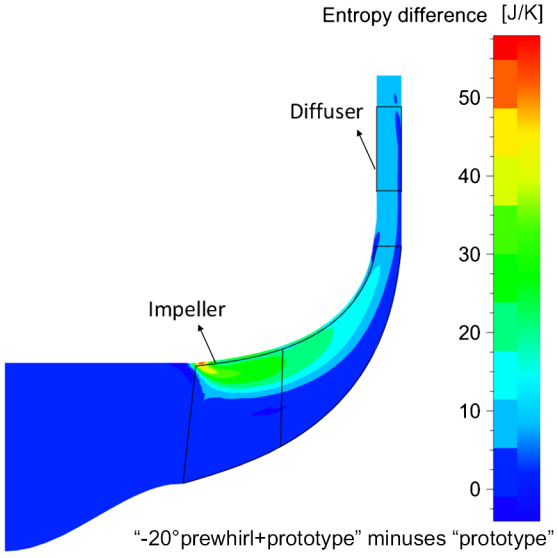

Fig. 19 Difference in entropy fields at the mass-flow rate of 0.24 kg/s.

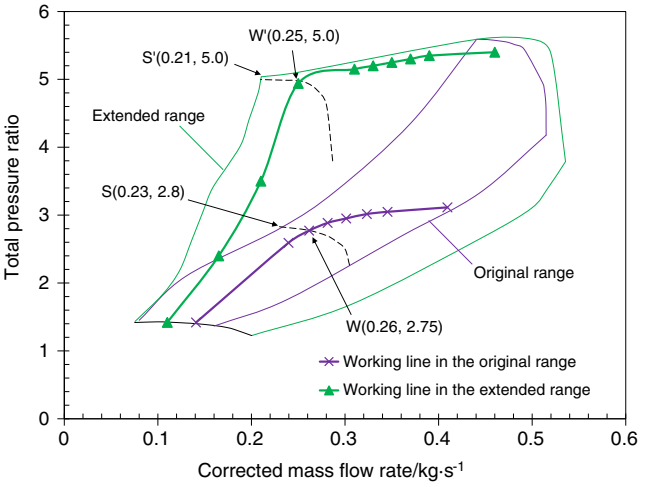

Fig. 20 Estimated working lines in the original range and the extended range.

critical SM. The PRs of W and W' can be used to estimate the improvement in the low-end torque.

$$\mathrm{SM} = \left(1 - \frac{\mathrm{PR}_w/\dot{m}_w}{\mathrm{PR}_s/\dot{m}_s}\right)_{N=\mathrm{const}} \times 100\% \tag{8}$$

Assuming that the mixture of air and fuel maintains its stoichiometry, the engine-shaft torque should be directly related to the amount of compressor intake. The ratio of pressures at W' and W is 1.82. If the compression process is assumed to be reversible and adiabatic, and the intercooling is neglected, the ratio of the air densities at W' and W is approximately 1.53 ($1.82^{1/\gamma}$, in which γ is 1.4). Assuming that the effective efficiency of the engine remains the same at W' and W, the ratio of the brake torques at W' and W should be the same as the ratio of the mixture amounts or the ratio of the intake amounts, as indicated by Eq. (9). Thus, with the variable-geometry method, the low-end torque of an engine is estimated to increase by 53%.

$$T_{\mathrm{tq}} = \frac{P_e}{w_s} = \frac{\eta_{\mathrm{et}}\dot{m}H_u}{\alpha w_s} \propto \mathrm{PR}^{1/\gamma} \tag{9}$$

V. Conclusions

To develop ultrahigh-power-density turbocharged engines, compressors are required to provide high-pressure air over a wide mass-flow range. The combination of the variable-inlet prewhirl and variable diffuser vanes was employed to extend the compressor operating range. Numerical simulations were used to investigate the performance of a centrifugal compressor with a diffuser-vane angle varying from −10 to 10 deg, and inlet prewhirl varying from −20 to 60 deg. The potentials of the combined method for extending the compressor operating range and improving low-end engine torque were estimated. The following conclusions are drawn:

1) Combining variable diffuser vanes, with angles between −10 and 10 deg, and variable-inlet prewhirl, between −20 and 60 deg, has the potential to improve the stable compressor operating range from 23.5 to 63.0% at a PR of 4.8. (Such a high PR can be a preferred choice for future turbocharged engines.) The shifts of the choke and surge lines contribute to this extension. The combination of positive inlet prewhirl and a closed diffuser has the advantage of moving the surge line left compared to only closing the diffuser or only using the positive inlet prewhirl. In addition to extending the flow range, another advantage of the variable-geometry method is its ability to achieve a higher-efficiency performance by adjusting the diffuser vane angle and prewhirl angle together.

2) For the prototype, at 60 and 40% speed, the influences of the inlet prewhirl on the surge flow and choking flow are negligible. For the case of closing the diffuser, even at 80 or 90% speed, the inlet prewhirl still has little effect. As indicated by the equations, if the original choking

Downloaded by TSINGHUA UNIVERSITY on October 11, 2017 | http://arc.aiaa.org | DOI: 10.2514/1.B36004

flow of a compressor is too small, the effect of the inlet prewhirl on shifting the characteristic will also be small. This is one of the reasons why the inlet prewhirl has little influence at low speeds.

3) When the relative Mach number in front of the inducer approaches unity, the relief of the relative Mach number by the positive inlet prewhirl will contribute significantly to stabilizing the performance of the impeller and moving the surge line to the left. This is another reason for the great displacement of the surge line at high speeds after employing the positive inlet prewhirl.

4) The inlet prewhirl does not always change the compressor choking mass-flow rates, which are influenced by impeller efficiency and work input. The positive inlet prewhirl reduces the work input from the impeller, but it may also contribute to improving impeller efficiency, which counteracts the drop in work input. The negative inlet prewhirl increases the work input, but it may worsen the performance improvements. The combined effects lead to no change in the compressor choking mass-flow rate.

5) Benefitting from the range extension of the compressor, the maximum pressure of intake for a turbocharged engine can be improved by approximately 82%, and the low-end torque is estimated to increase by 53%.

Acknowledgments

This research was supported by the National Natural Science Foundation of China (grant number 51176087). It was also sponsored by the State Key Laboratory of Automotive Safety and Energy under project number KF16102. The authors would like to thank the Institute of Jet Propulsion and Turbomachinery of the RWTH Aachen University for providing the test case, Radiver, a centrifugal compressor with a wedge diffuser.

References

[1] Smith, L. H., Jr., "NASA/GE Fan and Compressor Research Accomplishments," *Journal of Turbomachinery*, Vol. 116, No. 4, 1994, pp. 555–569.

[2] Whitfield, A., "Review of Variable Geometry Techniques Applied to Enhance the Performance of Centrifugal Compressors," *International Compressor Engineering Conference*, July 2000, Paper 2367.

[3] Ziegler, K. U., Justen, F., Rothstein, M., Gallus, H. E., and Niehuis, R., "Research on a Centrifugal Compressor of Variable Geometry," *International Compressor Engineering Conference*, July 2000, Paper 1371.

[4] Ubben, S., and Niehuis, R., "Experimental Investigation of the Diffuser Vane Clearance Effect in a Centrifugal Compressor Stage with Adjustable Diffuser Geometry—Part I: Compressor Performance Analysis," *Journal of Turbomachinery*, Vol. 137, No. 3, 2014, Paper 031003.

[5] Rodgers, C., "Turbocharging a High Altitude UAV C.I. Engine," AIAA Paper 2001-3970, July 2001.

[6] Aoyagi, Y., Kunishima, E., Asaumi, Y., Aihara, Y., Odaka, M., and Goto, Y., "Diesel Combustion and Emission Using High Boost and High Injection Pressure in a Single Cylinder Engine," *JSME International Journal, Series B: Fluids and Thermal Engineering*, Vol. 48, No. 4, 2005, pp. 648–655. doi:10.1299/jsmeb.48.648

[7] Blair, J., and Bower, G., "Development of a Miller Cycle Powersports Engine," Soc. of Automotive Engineers TP 2014-32-0090, 2014.

[8] Mohtar, H., Chesse, P., Yammine, A., and Hetet, J. F., "Variable Inlet Guide Vanes in a Turbocharger Centrifugal Compressor: Local and Global Study," Soc. of Automotive Engineers TP 2008-01-0301, 2008.

[9] Herbst, F., Stöber-Schmidt, C.-P., Eilts, P., Sextro, T., Kammeyer, J., Natkaniec, C., Seume, J., Porzig, D., and Schwarze, H., "The Potential of Variable Compressor Geometry for Highly Boosted Gasoline Engines," Soc. of Automotive Engineers TP 2011-01-0376, 2011.

[10] Coppinger, M., "Aerodynamic Performance of an Industrial Centrifugal Compressor Variable Inlet Guide Vane System," Ph.D. Dissertation, Loughborough Univ., Loughborough, England, U.K., 1999.

[11] Mohseni, A., Goldhahn, E., Van den Braembussche, R. A., and Seume, J. R., "Novel IGV Designs for Centrifugal Compressors and Their Interaction with the Impeller," *Journal of Turbomachinery*, Vol. 134, No. 2, 2012, Paper 021006. doi:10.1115/1.4003235

[12] Galindo, J., Serrano, J. R., Margot, X., Tiseira, A., Schorn, N., and Kindl, H., "Potential of Flow Pre-Whirl at the Compressor Inlet of Automotive Engine Turbochargers to Enlarge Surge Margin and Overcome Packaging Limitations," *International Journal of Heat and Fluid Flow*, Vol. 28, No. 3, 2007, pp. 374–387. doi:10.1016/j.ijheatfluidflow.2006.06.002

[13] Sezal, I., Lang, M., Aalburg, C., Chen, N., Erhard, W., Greco, A. S. D., Tapinassi, L., and Gadamsetty, R. K., "Introduction of Circumferentially Non-Uniform Variable Guide Vanes in the Inlet Plenum of a Centrifugal Compressor for Minimum Losses and Flow Distortion," *Journal of Turbomachinery*, Vol. 138, No. 9, 2016, Paper 091008.

[14] Kyrtatos, N., and Watson, N., "Application of Aerodynamically Induced Prewhirl to a Small Turbocharger Compressor," *Journal of Engineering for Power*, Vol. 102, No. 4, 1980, pp. 943–950. doi:10.1115/1.3230365

[15] Whitfield, A., and Abdullah, A. H., "The Performance of a Centrifugal Compressor with High Inlet Prewhirl," *Journal of Turbomachinery*, Vol. 120, No. 3, 1998, pp. 487–493. doi:10.1115/1.2841744

[16] Oatway, T. P., and Harp, J. L., "Investigations of a Variable Geometry Compressor for a Diesel Engine Turbocharger," U.S. Army Tank-Automotive Command Rept. SR-21, Warren, MI, 1973.

[17] Jiao, K., Sun, H., Li, X., Wu, H., Krivitzky, E., Schram, T., and Larosiliere, L. M., "Numerical Investigation of the Influence of Variable Diffuser Vane Angles on the Performance of a Centrifugal Compressor," *Proceedings of the Institution of Mechanical Engineers, Part D: Journal of Automobile Engineering*, Vol. 223, No. 8, 2009, pp. 1061–1070.

[18] Simon, H., Wallmann, T., and Monk, T., "Improvements in Performance Characteristics of Single-Stage and Multistage Centrifugal Compressors by Simultaneous Adjustments of Inlet Guide Vanes and Diffuser Vanes," *Journal of Turbomachinery*, Vol. 109, No. 1, 1987, pp. 41–47. doi:10.1115/1.3262068

[19] Zheng, X., and Huang, Q., "Potential of the Range Extension of Compressors with a Variable Inlet Prewhirl for Automotive Turbocharged Engines with an Ultra-High-Power Density," *Proceedings of the Institution of Mechanical Engineers, Part D: Journal of Automobile Engineering*, Vol. 229, No. 14, 2015, pp. 1959–1968.

[20] Zheng, X., Huenteler, J., Yang, M., Zhang, Y., and Bamba, T., "Influence of the Volute on the Flow in a Centrifugal Compressor of a High-Pressure Ratio Turbocharger," *Proceedings of the Institution of Mechanical Engineers, Part A: Journal of Power and Energy*, Vol. 224, No. 7, 2010, pp. 1157–1159. doi:10.1177/095440541022400702

[21] Anon., *User Manual*, FINE/Turbo v8.7, NUMECA International, Brussels, Belgium, 2010, pp. 9–11, Chap. 4.

[22] Ziegler, K. U., Gallus, H. E., and Niehuis, R., "A Study on Impeller–Diffuser Interaction—Part I: Influence on the Performance," *Journal of Turbomachinery*, Vol. 125, No. 1, 2003, pp. 173–182. doi:10.1115/1.1516814

[23] Zheng, X., Huang, Q., and Liu, A., "Loss Mechanisms and Flow Control for Improved Efficiency of a Centrifugal Compressor at High Inlet Prewhirl," *Journal of Turbomachinery*, Vol. 138, No. 10, 2016, pp. 101011–101011. doi:10.1115/1.4033216

[24] Huang, Q., Zheng, X., and Wang, A., "Mechanism and Flow Control on the Mismatching of Impeller and Vaned Diffuser Caused by Inlet Prewhirl for Centrifugal Compressors," *Turbo Expo*, American Soc. of Mechanical Engineers Paper GT2016-56244, Seoul, South Korea, 2016.

[25] Casey, M., and Rusch, D., "The Matching of a Vaned Diffuser with a Radial Compressor Impeller and Its Effect on the Stage Performance," *Journal of Turbomachinery*, Vol. 136, No. 12, 2014, pp. 121004–121004. doi:10.1115/1.4028218

[26] Cumpsty, N. A., *Compressor Aerodynamics*, Kreiger, Malabar, FL, 2004, pp. 4, 107, 367.

[27] Rodgers, C., "Centrifugal Compressor Inlet Guide Vanes for Increased Surge Margin," *Journal of Turbomachinery*, Vol. 113, No. 4, 1991, pp. 696–702. doi:10.1115/1.2929136

[28] Senoo, Y., Hayami, H., Kinoshita, Y., and Yamasaki, H., "Experimental Study on Flow in a Supersonic Centrifugal Impeller," *Journal of Engineering for Power*, Vol. 101, No. 1, 1979, pp. 32–39. doi:10.1115/1.3446453

F. Liu
Associate Editor

Downloaded by TSINGHUA UNIVERSITY on October 11, 2017 | http://arc.aiaa.org | DOI: 10.2514/1.B36004